SIMILARITIES BETWEEN GUIDED LONGITUDINAL ULTRASONIC WAVES IN TUBES AND PLATES

Mihai Valentin PREDOI[1], Andreea-Denisa GRIGUȚA[2], Cristian Cătălin PETRE[3]

Guided waves in hollow cylinders have been theoretically investigated for more than fifty years. The dispersion equations for the longitudinal waves L(0,n) have been numerically solved by many authors and even commercial software exist to provide numerical solutions for a given practical case. A numerical coincidence of the dispersion curves of the longitudinal waves propagating along a hollow cylinder and those of the Lamb waves propagating in plates has been remarked by many authors. However this coincidence is valid only in the high frequency range, whereas for very low frequencies, only L(0,1) mode is propagating and L(0,2) mode has a cut-off frequency. These properties of the longitudinal guided waves in tubes are analytically investigated in this paper, analytically proving the asymptotic convergence of the dispersion curves at high frequencies towards those of Lamb guided waves in plates. Then, the cut-off frequency of L(0,2) mode in pipes is determined using a simple analytical formula and an investigation of the imaginary and complex branches below this cut-off concludes the paper.

Keywords: Tube guided waves, Lamb waves

1. Introduction

Guided waves in plates for stress free boundary conditions have been investigated by Lamb [1] who deduced the dispersion equations of the nowadays called, symmetrical (S) and anti-symmetrical (A) Lamb waves. The complex or imaginary parts of the dispersion curves and their cut-off frequencies are presented in many textbooks on ultrasonic waves (see e.g., ref. [2], [3]).

A first theoretical investigation of propagating waves along pipes, including numerical solutions of the dispersion curves was done by Gazis [4], [5]. Waves propagating in circumferential direction were investigated among others by Heimann and Kolsky [6], but these waves are not in the scope of the present paper.

Measurements of the group velocities for the first four longitudinal modes in a tube were done by Fitch [7]. He mistakenly considers that the first two

[1] Prof., Department of Mechanics, Fac. I.S.B, University POLITEHNICA of Bucharest, Romania, e-mail: mihai.predoi@upb.ro
[2] Eng., Stud., Faculty of Biotechnical Systems Engineering, University POLITEHNICA of Bucharest, Romania, e-mail: griguta_andreea_denisa@yahoo.com
[3] Prof., Department of Strength of Materials, University POLITEHNICA of Bucharest, Romania, e-mail: cristian.petre@upb.ro

longitudinal modes are propagating at all frequencies, but remarks the measured coincidence of the group velocities of the first symmetric mode S_0 in a plate and the L(0,2) mode in the pipe.

Li and Rose [8], confronted with the more complicated dispersion equations for pipes, have used instead the dispersion equations of the Lamb waves for plates. They remark the existence of a "low frequency" domain in which plate and tube dispersion curves are totally different, but at higher frequencies an almost perfect coincidence of phase velocities of plates and pipes is presented. Velichko and Wilcox approximate the guided waves in thin walled pipes by shell theories, their results having applicability only for wavelengths considerably less than the pipe circumference [9]. A much more accurate numerical investigation of the phase velocity of the L(0,1) mode in the low frequency range, for several wall thicknesses to radius ratios is shown by Ratassepp et al. in [10]. The complex branches of the dispersion curves are also presented, but they are missing the imaginary branches. The numerical convergence of the tube dispersion curves towards those of plates has been presented also by Predoi et al. [11].

The present work begins with an analytical approach, proving the asymptotic convergence of the L(0,n) dispersion in tubes, towards the Lamb waves dispersion curves in plates, for increasing frequencies. The convergence is more rapid for smaller thickness to radius ratios. The cut-off frequency for the L(0,2) mode, overlooked by many authors, is analytically deduced as a simple to use formula. Dispersion curves are plotted also in the complex plane with emphasis to the low frequency range, in which the imaginary branches are separated among the modes, a fact which is missing in many other researches.

2. Theoretical aspects

2.1. Dispersion equation for the plate in vacuum

The geometry for the plate and pipe is presented on Fig. 1. The material is isotropic and homogeneous for both the plate and the pipe, defined by Lamé constants (λ, μ) and the mass density ρ. Thus, the velocities of the bulk longitudinal and transversal waves are given by $c_L^2 = (\lambda + \mu)/\rho$ and respectively by $c_T^2 = \mu/\rho$. The corresponding bulk wavenumbers are $k_L = \omega / c_L$ and respectively $k_T = \omega / c_T$ in which ω is the angular frequency $\omega = 2\pi f$ for a given frequency *f*. Consequently the Lamé constants (parameters) can be expressed as:

$$\mu = \rho c_T^2;\ \lambda = \rho\left(c_L^2 - 2c_T^2\right) \tag{1}$$

The plate has a thickness *2h* and ultrasonic wave propagation is along the Oz axis, which is placed in the middle/symmetry plane of the plate. The tube has a

mean radius *R*, from which the outer and inner cylindrical surfaces are distanced by *h*, for a better analogy.

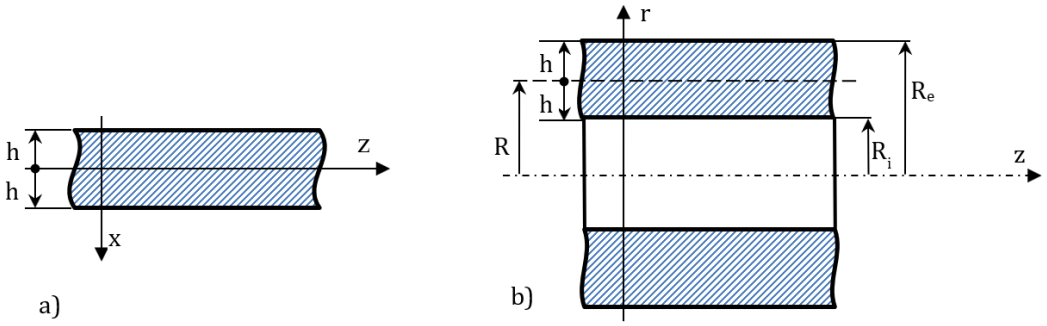

Fig. 1 Geometry of the plate (a) and of the tube (b)

On the two parallel free surfaces of the plate, the normal and shear stresses for a plate in vacuum must cancel for any position z. Following the notations used by Viktorov [1], these boundary conditions lead to a homogeneous linear system of four equations and four unknowns. Using the notations $p^2 = k_L^2 - k^2$ and $q^2 = k_T^2 - k^2$ in which k is the wavenumber of the guided waves, the associated determinant must cancel for a non-trivial solution, that is [1]:

$$\begin{vmatrix} \left(k^2-q^2\right)cos\left(ph\right) & 2ikqcos\left(qh\right) & 0 & 0 \\ 2ikpsin\left(ph\right) & \left(k^2-q^2\right)sin\left(qh\right) & 0 & 0 \\ 0 & 0 & \left(k^2-q^2\right)sin\left(qh\right) & 2ikqsin\left(qh\right) \\ 0 & 0 & 2ikpcos\left(ph\right) & \left(k^2-q^2\right)cos\left(qh\right) \end{vmatrix} = 0 \qquad (2)$$

The two minor determinants on the upper left and lower right, cancel for the wavenumbers of the symmetrical (S) and respectively anti-symmetrical (A) modes of a homogeneous isotropic plate. For more detail, see references [2], [3], [12].

2.2 Dispersion equation for the cylindrical pipe in vacuum. Convergence towards the plate dispersion equation.

The axially symmetric $\frac{\partial \cdot}{\partial \theta} \equiv 0$ longitudinal waves in a pipe are defined in cylindrical coordinates (r,θ,z). The scalar potential is $\varphi\left(r,\theta,z,t\right)$ and from the vector potential $\overline{\Psi}\left(r,\theta,z,t\right)$ is selected only the non-zero component $\Psi_\theta\left(r,\theta,z,t\right)$, which are both verifying the corresponding wave equations in cylindrical coordinates:

$$\frac{\partial^2\varphi}{\partial r^2}+\frac{1}{r}\frac{\partial\varphi}{\partial r}+\frac{\partial^2\varphi}{\partial z^2}=\frac{1}{c_L^2}\frac{\partial^2\varphi}{\partial t^2};$$
$$\frac{\partial^2\Psi_\theta}{\partial r^2}+\frac{1}{r}\frac{\partial\Psi_\theta}{\partial r}-\frac{\Psi_\theta^2}{r^2}+\frac{\partial^2\Psi_\theta}{\partial z^2}=\frac{1}{c_L^2}\frac{\partial^2\Psi_\theta}{\partial t^2} \tag{3}$$

The general solutions can be expressed using Bessel functions of first kind $J_0(z), J_1(z)$ and of second kind $Y_0(z), Y_1(z)$, using the same notations for p and q as for the plate [4]:

$$\varphi(r,z,t)=\left[A_1J_0(pr)+A_2Y_0(pr)\right]\exp\left[i(kz-\omega t)\right]$$
$$\Psi_\theta(r,z,t)=\left[B_1J_1(qr)+B_2Y_1(qr)\right]\exp\left[i(kz-\omega t)\right] \tag{4}$$

The radial and axial displacements can be obtained from their definitions:

$$u_r=\frac{\partial\varphi}{\partial r}-\frac{\partial\Psi_\theta}{\partial z};\quad u_z=\frac{\partial\varphi}{\partial z}+\frac{\partial\Psi_\theta}{\partial r}+\frac{\Psi_\theta}{r} \tag{5}$$

Using the strain expressions in cylindrical coordinates and the linear elasticity constitutive law, the radial stress and the radial-axial shear stresses can be written:

$$\sigma_{rr}=(\lambda+2\mu)\frac{\partial^2\varphi}{\partial r^2}+\lambda\left(\frac{1}{r}\frac{\partial\varphi}{\partial r}+\frac{\partial^2\varphi}{\partial z^2}\right)-2\mu\frac{\partial^2\Psi_\theta}{\partial r\partial z}$$
$$\sigma_{rz}=\frac{\mu}{2}\left(2\frac{\partial^2\varphi}{\partial r\partial z}+\frac{\partial^2\Psi_\theta}{\partial r^2}+\frac{1}{r}\frac{\partial\Psi_\theta}{\partial r}-\frac{\Psi_\theta}{r^2}-\frac{\partial^2\Psi_\theta}{\partial z^2}\right) \tag{6}$$

Injecting the potentials (4) in the previous expressions and leaving aside the common propagating factor $\exp\left[i(kz-\omega t)\right]$, one gets from (6):

$$\frac{\sigma_{rr}}{\mu}=A_1\left[\left(k^2-q^2\right)J_0(pr)+2\frac{p}{r}J_1(pr)\right]+A_2\left[\left(k^2-q^2\right)Y_0(pr)+2\frac{p}{r}Y_1(pr)\right]$$
$$+B_1 2ik\left[qJ_0(qr)-\frac{1}{r}J_1(qr)\right]+B_2 2ik\left[qY_0(qr)-\frac{1}{r}Y_1(qr)\right]$$
$$2\frac{\sigma_{rz}}{\mu}=-2ikpA_1J_1(pr)-2ikpA_2Y_1(pr)+B_1\left(q^2-k^2\right)J_1(qr)+B_2\left(q^2-k^2\right)Y_1(qr) \tag{7}$$

The dispersion equation is obtained by imposing stress free boundary conditions at $r_{1,2}=R\pm h$, for stresses defined by eq. (7). A homogeneous algebraic

system of four equations is thus obtained [4],…, [10] and by adequate numerical methods, the dispersion curves *(k,ω)* can be obtained for a cylindrical tube.

In order to prove that for large radius *R* and high frequency, these equations coincide with equations (1), the first step is to take to the limit all terms containing the factor $1/(R\pm h)$ in the radial stress equation, for $R\to\infty$. The Bessel functions from (7), can be approximated for large arguments ($|z|\to\infty$) by the following analytical functions (see ref. [12]):

$$\begin{aligned} J_0(z)&=\sqrt{\frac{2}{\pi z}}\cos\left(z-\frac{\pi}{4}\right);\ Y_0(z)=\sqrt{\frac{2}{\pi z}}\sin\left(z-\frac{\pi}{4}\right)\\ J_1(z)&=\sqrt{\frac{2}{\pi z}}\sin\left(z-\frac{\pi}{4}\right);\ Y_0(z)=-\sqrt{\frac{2}{\pi z}}\cos\left(z-\frac{\pi}{4}\right)\end{aligned} \tag{8}$$

Developing the trigonometric functions, and grouping the functions with identical arguments, one gets, using the following coefficients, $\hat{A}_1=A_1-A_2$, $\hat{A}_2=A_1+A_2$, $\hat{B}_1=B_1-B_2$, $\hat{B}_2=B_1+B_2$:

$$\begin{aligned} \frac{\sqrt{\pi}\sigma_{rr}}{\mu}&=\frac{k^2-q^2}{\sqrt{pR}}\left\{\hat{A}_1\cos\left[p(R\pm h)\right]+\hat{A}_2\sin\left[p(R\pm h)\right]\right\}\\ &\quad+\frac{2ikq}{\sqrt{qR}}\left\{\hat{B}_1\cos\left[q(R\pm h)\right]+\hat{B}_2\sin\left[q(R\pm h)\right]\right\}=0\\ 2\frac{\sqrt{\pi}\sigma_{rz}}{\mu}&=\frac{2ikp}{\sqrt{pR}}\left\{\hat{A}_1\sin\left[p(R\pm h)\right]-\hat{A}_2\cos\left[p(R\pm h)\right]\right\}\\ &\quad+\frac{k^2-q^2}{\sqrt{qR}}\left\{\hat{B}_1\sin\left[q(R\pm h)\right]-\hat{B}_2\cos\left[q(R\pm h)\right]\right\}=0\end{aligned} \tag{9}$$

The determinant of the homogeneous algebraic system (9) can be multiplied by $\sqrt{pR}\neq 0$ along the first two columns and by $\sqrt{qR}\neq 0$ along the last two columns, obtaining thus:

$$\begin{vmatrix} (k^2-q^2)(c_1y_1-s_1x_1) & (k^2-q^2)(c_1x_1+s_1y_1) & 2ikq(c_2y_2-s_2x_2) & 2ikq(c_2x_2+s_2y_2)\\ (k^2-q^2)(c_1y_1+s_1x_1) & -(k^2-q^2)(c_1x_1-s_1y_1) & 2ikq(c_2v+s_2x_2) & -2ikq(c_2x_2-s_2y_2)\\ 2ikp(c_1x_1+s_1y_1) & -2ikp(c_1y_1-s_1x_1) & (k^2-q^2)(c_2x_2+s_2y_2) & -(k^2-q^2)(c_2y_2-s_2x_2)\\ -2ikp(c_1x_1-s_1y_1) & -2ikp(c_1y_1+s_1x_1) & -(k^2-q^2)(c_2x_2-s_2y_2) & -(k^2-q^2)(c_2y_2+s_2x_2)\end{vmatrix}=0 \tag{10}$$

The following notations have been used, for briefness:

$$\begin{aligned} &s_1=\sin pR;\ c_1=\cos pR;\ s_2=\sin qR;\ c_2=\cos qR\\ &x_1=\sin ph;\ y_1=\cos ph;\ x_2=\sin qh;\ y_2=\cos qh\end{aligned} \tag{11}$$

After several transformations of the determinant (10), as presented in the Annex, it is proven the analytical convergence of the dispersion equations for a plate (2) and a cylindrical tube (10), having the same wall thickness, as long as the asymptotic formulas (8) hold, that is for large R/h ratios:

$$\begin{vmatrix} \left(k^2-q^2\right)\cos ph & 2ikq\cos qh & 0 & 0 \\ 2ikp\sin ph & \left(k^2-q^2\right)\sin qh & 0 & 0 \\ 0 & 0 & 2ikp\cos ph & -\left(k^2-q^2\right)\cos qh \\ 0 & 0 & \left(k^2-q^2\right)\sin ph & -2ikq\sin qh \end{vmatrix} = 0 \quad (12)$$

3. Numerical examples

As a first numerical example, is taken a standard 25.4mm (1 inch) diameter pipe, R_e=16.7 mm, R_i=13.3 mm, R_i/R_e=0.8, h=1.7mm, the half wall thickness, or h/R=0.111 (the mean radius is R=15mm) and comparison is made with a plate of the same h=1.7 mm as half plate thickness. The material for both structures is steel: ρ=7850 kg/m^3, c_L= 6089 m/s, c_T=3195 m/s. Using formulas (1) : λ=130.8 GPa and μ=80.133 GPa.

For a wider applicability, instead of the frequency f or angular frequency $\omega = 2\pi f$, in the following figures are used the non-dimensional frequency $\Omega = \omega h/c_T$ and the non-dimensional wavenumber kh (Fig. 2a).

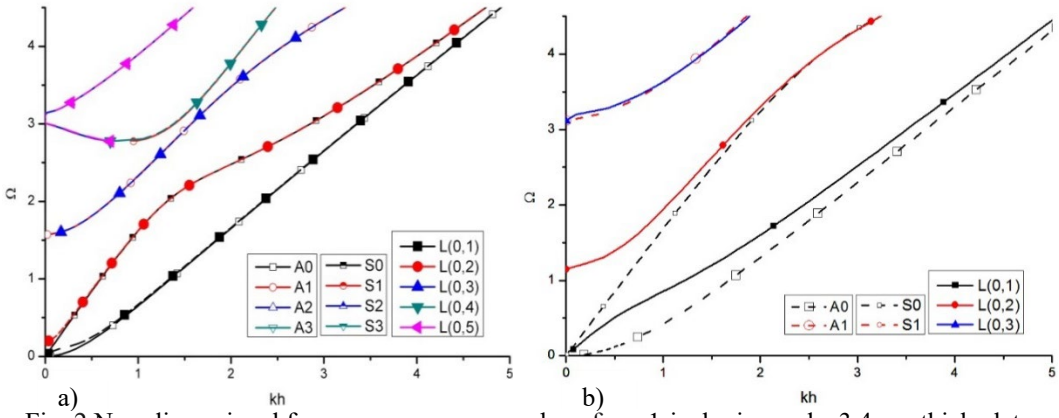

Fig. 2 Non-dimensional frequency vs. wavenumbers for a 1-inch pipe and a 3.4mm thick plate, both made of steel Ri/Re=0.8 (a), Ri/Re=0.5 (b). Markers are 'full' for pipe, 'hollow' for antisymmetric modes and 'half-full' for symmetric plate modes. (Color online)

All curves are numerical solutions of dispersion equations (2) and (10) using numerical methods developed by the authors using an algorithm described in ref. [14] and the eigenvalue solver of COMSOL [15].

The axially symmetric L(0,2) mode (red dots) converges at frequencies above its cut-off frequency, towards the symmetrical S_0 mode (black half squares) of the plate. The L(0,1) mode (black full squares) at very low frequencies is close to the S_0 mode (black half squares) but is separating from this mode, as the frequency increases and tends towards the plate fundamental anti-symmetric mode A_0 (black squares) as the frequency is $\Omega > 0.3$. All the higher order modes of the cylindrical tube, coincide with those of the plate beginning from their respective cut-off frequencies (Fig. 2a). Even in the low frequency range ($\Omega<1$), the L(0,3) mode is practically superposed onto the A_1 plate mode. This remark can be extended for higher order modes: L(0,4) tends to S_1 , L(0,5) tends to S_2, etc. Replacement of pipe dispersion curves by Lamb dispersion curves as it is shown on Fig. 2a looks as a very good approximation. In order to see the limits of such approximation, a second example is given.

In this second example (Fig. 2b) is considered a pipe made of the same material, with geometrical parameters: R_e=16.7 mm, R_i=8.35 mm, R_i / R_e=0.5, h=4.175 mm, the half wall thickness, or h/R=0.333 (the mean radius R= 12.525 mm). In this case, there is a noticeable discrepancy between the curves representing the mode L(0,1) and L(0,2) and their corresponding Lamb modes in plates, especially for thicker pipes, as shown on Fig. 2b, and this aspect is discussed in the following section.

4. Accuracy of the L(0,1) and L(0,2) tube modes replacement by Lamb plate modes at low frequencies

Many authors indicate that dispersion curves of plates can replace those for L(0,n) modes in thin tubes. However, it is interesting to quantitatively estimate this statement, since there is no systematic investigation to date of the error made by replacing the first two modes of the pipe with those of the plate. The first two modes are investigated in the low Ω frequency range for three R_i/R_e ratios, namely 0.5, 0.7 and 0.9, or $h/R \in \{0.333 \quad 0.176 \quad 0.053\}$.

As expected, thinner tubes have faster converging dispersion curves towards the corresponding plate dispersion curves (Fig. 3). A 5% error in kh non-dimensional wavenumber of the L(0,2) mode, is obtained for $\Omega > 0.15$ if Ri/R_e=0.9, but only for $\Omega >2.2$ if Ri/R_e=0.5. The L(0,1) mode has higher approximation errors, as the frequency increases, than those of the L(0,2) convergence towards the S_0 mode. In fact, the L(0,2) mode approximation by the S_0 mode can only be considered after its cut-off frequency because at the cut-off frequency there is a vertical asymptote in these approximations. This aspect motivates the study of the L(0,2) mode cut-off in the next section.

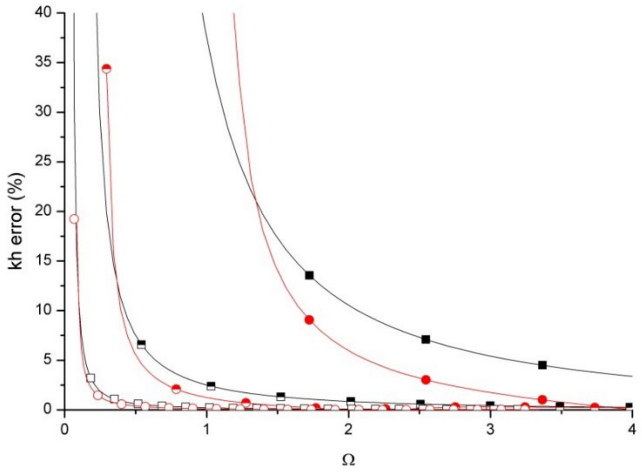

Fig. 3 Error (%) in the non-dimensional *kh* wavenumber caused by replacing the L(0,1) (squares) and L(0,2) (circles) dispersion curves, by the A0 and S0 dispersion curves respectively as function of $\Omega = \omega h/c_T$, for *Ri/Re=0.5* (full markers), *Ri/Re=0.7* (half-full markers)

5. Analytical formula for the cut-off frequency of the L(0,2) mode

For very low frequencies, the L(0,2) becomes propagative at frequencies above a specific cut-off frequency, which was not investigated before, to our knowledge. The cut-off equation is obtained by setting $k=0$ in the equations cancelling mechanical stresses (7), for $\omega=0$ in which case $p=k_L$, $q=k_T$: The determinant reduces in this case to a product of the following two determinants.

$$\begin{vmatrix} -\omega J_0\left(\frac{\omega R_e}{c_L}\right)+2\frac{c_T^2}{c_L R_e}J_1\left(\frac{\omega R_e}{c_L}\right) & -\omega Y_0\left(\frac{\omega R_e}{c_L}\right)+2\frac{c_T^2}{c_L R_e}Y_1\left(\frac{\omega R_e}{c_L}\right) \\ -\omega J_0\left(\frac{\omega R_i}{c_L}\right)+2\frac{c_T^2}{c_L R_i}J_1\left(\frac{\omega R_i}{c_L}\right) & -\omega Y_0\left(\frac{\omega R_i}{c_L}\right)+2\frac{c_T^2}{c_L b}Y_1\left(\frac{\omega R_i}{c_L}\right) \end{vmatrix} = 0;$$
$$\begin{vmatrix} J_1\left(\frac{\omega}{c_T}R_e\right) & Y_1\left(\frac{\omega}{c_T}R_e\right) \\ J_1\left(\frac{\omega}{c_T}R_i\right) & Y_1\left(\frac{\omega}{c_T}R_i\right) \end{vmatrix} = 0. \qquad (13)$$

The outer radius $R_e = R + h$ and the inner radius $R_i = R - h$, are used for shorter formulas (as defined on Fig. 1). Obviously the first root, coming from eq. (12) is $\omega=0$, which means there is no cut-off for the L(0,1) mode.

The second cut-off frequency is obtained also from the first equation (12), then the next one from the second determinant of (12) and so on. These cut-offs are plotted on Fig. 4.

It is useful to determine the first cut-off frequency, preferably by an analytical formula. Indeed, for small arguments (z<<1) the following approximations hold [13]:

$$J_0(z) \approx 1;\ J_1(z) \approx \frac{z}{2};\ Y_0(z) \approx \frac{2}{\pi}\ln z;\ Y_1(z) \approx -\frac{2}{\pi z} \tag{14}$$

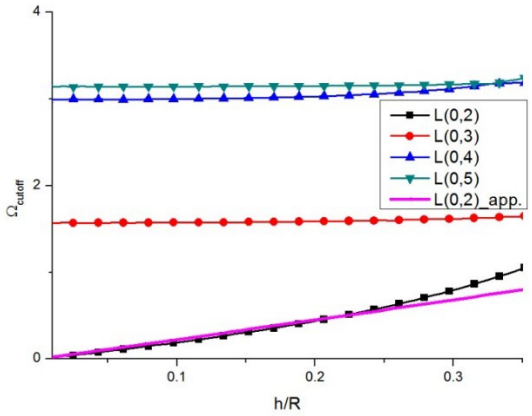

Fig. 4 Non-dimensional cut-off frequencies vs. relative thickness h/Re for tubes made of steel and approximate analytical formula (L(0,2)_app, with no marker), (Color online).

The first determinant of (12) can be asymptotically transformed, based on these approximations and the following formula is thus obtained:

$$\Omega = \frac{h}{R}\left(2 + \frac{1}{8}\frac{h}{R}\right), \tag{15}$$

in which the same notations as in Fig. 1 were used. The results from the application of this simple formula are plotted on the same Fig. 4 and agree well with the exact values (obtained by numerical methods) up to h/R=0.3, which is the upper limit of almost all thick pipes commonly used in practice. As the relative thickness tends to zero, the plate case is obtained (Ω=0), for which the S_0 mode has no cut-off frequency.

6. Detail on the dispersion curves of pipes below the first cut-off frequency

Most papers considering longitudinal modes L(0,n) propagation, are more or less vague about the dispersion curves below the first cut-off frequency. The explanation comes from the numerical difficulties in accurately solving the dispersion equation (10).

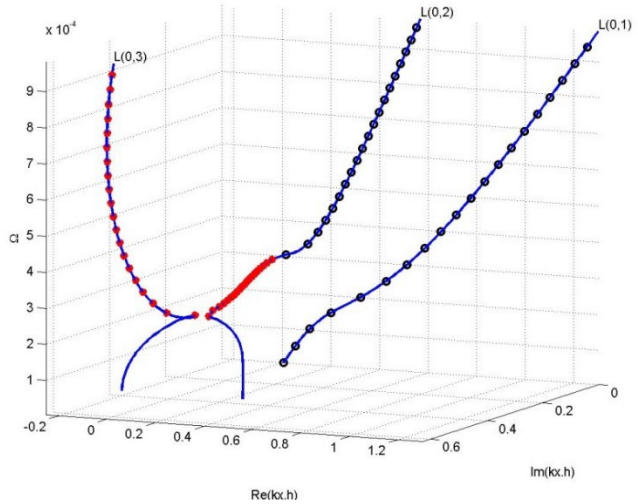

Fig. 5 Dispersion curves of the first three modes as Ω vs real(kh) and imag(kh). Real branches (blue circles), imaginary branch (red dots), complex branches (solid line). (Color online).

The numerical results are obtained using the algorithm described in ref. [14], and the eigenvalue solver of COMSOL [15]. The dispersion curves presented on Fig. 5, are for a tube of Ri/R_e=0.7, made of the same steel material. The first three modes are plotted as Ω vs. the real and imaginary parts of *kh*. The L(0,1) mode has only real wavenumbers. L(0,2) begins as a complex valued wavenumber (blue line) and becomes purely imaginary (red dots) before its cut-off frequency. The L(0,3) mode begins with L(0,2) values mirrored by the zero real-wavenumber plane, having the same imaginary part, but negative real part. L(0,3) and L(0,2) mode change to imaginary wavenumbers at the same frequency. From this frequency upwards, the L(0,3) mode has increasing imaginary values (red dots) for the wavenumber, which correspond to high wave attenuation, before becoming propagative for a higher cut-off frequency (see Fig.2b). This topological structure has been found for all investigated thicknesses, representing an important result of the present work.

5. Conclusions

Dispersion curves of tubes in vacuum have been investigated and the asymptotical convergence of the dispersion equations towards the dispersion equations of plates in vacuum has been analytically proven. The relative errors in non-dimensional wave numbers, due the use of plate equations instead of tube equations are also computed, with recommendations on accuracy, depending on pipe wall thickness. The cut-off frequency of the L(0,2) mode is then determined by an asymptotically deduced analytical formula, which is compared against the accurate numerical values. The imaginary and complex branches of the L(0,2) mode below the cut-off

frequency are numerically determined. The specific real, imaginary or complex branches of the first three guided modes in this frequency range are labelled for each mode. All computations are done for steel pipes and for a wide technical range of wall thickness vs. mean radius.

REFERENCES

[1] *I. A. Viktorov,* Rayleigh and Lamb waves, New York: Plenum Press, 1967.

[2] *J. D. Achenbach*, Wave propagation in elastic solids, Amsterdam: North Holland, 1973.

[3] *K. F. Graff*, Wave Motion in Elastic Solids, New York: Dover Publ., 1975.

[4] *D. C. Gazis*, "Three-Dimensional Investigation of the Propagation of Waves in Hollow Circular Cylinders. I. Analytical Foundation," *The Journal of the Acoustical Society of America,* vol. 31, no. 5, pp. 568-573, 1959.

[5] *D. C. Gazis*, "Three-Dimensional Investigation of the Propagation of Waves in Hollow Circular Cylinders. II. Numerical Results," *The Journal of the Acoustical Society of America,* vol. 31, no. 5, pp. 573-578, 1959.

[6] *J. H. Heimann and H. Kolsky*, "The propagation of elastic waves in thin cylindrical shells," *Journal of the Mechanics and Physics of Solids,* vol. 14, pp. 121-130, 1966.

[7] *A. H. Fitch,* "Observation of elastic-pulse propagation in axially symmetric and nonaxially symmetric longitudinal modes of hollow cylinders," *J. Acoust. Soc. Am.,* vol. 35, no. 5, pp. 706-708, 1963.

[8] *J. Li and J. L. Rose*, "Excitation and propagation of non-axisymmetric guided waves in a hollow cylinder," *The Journal of the Acoustical Society of America,* vol. 109, no. 2, pp. 457-464, February 2001.

[9] *A. Velichko and P. D. Wilcox*, "Excitation and scattering of guided waves: Relationships between solutions for plates and pipes," *The Journal of the Acoustical Society of America,* vol. 125, no. 6, p. 3623–3631, 2009.

[10] *M. Ratassepp, A. Klauson, F. Chati, F. Leon and G. Maze*, "Edge resonance in semi-infinite thick pipe: Numerical predictions and measurements," *The Journal of the Acoustical Society of America,* vol. 124, no. 2, pp. 875-885, 2008.

[11] *M. V. Predoi, C. C. Petre and J. -. L. Izbicki*, "Fluid Structure Coupling in Guided Modes of Thin Pipes," in *IEEE International Ultrasonics Symposium*, Dresden, 2012.

[12] *M. V. Predoi and C. C. Petre*, Controle par ultrasons des plaques soudees, Bucharest: Ed. Printech, 2003, p. 150.

[13] *M. Abramowitz and I. Stegun*, Handbook of Mathematical Functions, New York: Dover Publications, 1964.

[14] *M. V. Predoi,* "Guided waves dispersion equations for orthotropic multilayered pipes solved using standard finite elements code," *Ultrasonics,* vol. 54, no. 7, pp. 1825-1831, 2014.

[15] "COMSOL Multiphysics Modeling Software," 2016. [Online]. [Accessed 2016].

ANNEX

Detailed transformations of the determinant (10) with notations (11) representing the dispersion equation for a tube, towards the determinant (2) corresponding to plates, are given in the following.

Linear combinations like half the sum and difference of the first two and respectively last two rows lead to:

$$\begin{vmatrix} \left(k^2-q^2\right)c_1y_1 & \left(k^2-q^2\right)s_1y_1 & 2ikqc_2y_2 & 2ikqs_2y_2 \\ \left(k^2-q^2\right)s_1x_1 & -\left(k^2-q^2\right)c_1x_1 & 2ikqs_2x_2 & -2ikqc_2x_2 \\ 2ikps_1y_1 & -2ikpc_1y_1 & \left(k^2-q^2\right)s_2y_2 & -\left(k^2-q^2\right)c_2y_2 \\ 2ikpc_1x_1 & 2ikps_1x_1 & \left(k^2-q^2\right)c_2x_2 & \left(k^2-q^2\right)s_2x_2 \end{vmatrix} = 0 \qquad (1)$$

Permuting second and third columns and the second and fourth rows, one gets:

$$\begin{vmatrix} \left(k^2-q^2\right)c_1y_1 & 2ikqc_2y_2 & \left(k^2-q^2\right)s_1y_1 & 2ikqs_2y_2 \\ 2ikpc_1x_1 & \left(k^2-q^2\right)c_2x_2 & 2ikps_1x_1 & \left(k^2-q^2\right)s_2x_2 \\ 2ikps_1y_1 & \left(k^2-q^2\right)s_2y_2 & -2ikpc_1y_1 & -\left(k^2-q^2\right)c_2y_2 \\ \left(k^2-q^2\right)s_1x_1 & 2ikqs_2x_2 & -\left(k^2-q^2\right)c_1x_1 & -2ikqc_2x_2 \end{vmatrix} = 0 \qquad (2)$$

An equivalent determinant is obtained by adding to the first two columns multiplied by c_1 and respectively c_2, the third column multiplied by s_1 and respectively the last one multiplied by s_2. The last two columns of multiplied $-c_1$ and respectively $-c_2$ are summed with the first two rows of the above formula multiplied by s_1 and respectively s_2. The determinant with initial notations becomes:

$$\begin{vmatrix} \left(k^2-q^2\right)\cos ph & 2ikq\cos qh & 0 & 0 \\ 2ikp\sin ph & \left(k^2-q^2\right)\sin qh & 0 & 0 \\ 0 & 0 & 2ikp\cos ph & -\left(k^2-q^2\right)\cos qh \\ 0 & 0 & \left(k^2-q^2\right)\sin ph & -2ikq\sin qh \end{vmatrix} = 0 \qquad (3)$$

This form of the determinant is obviously equivalent to (2), proving thus the coincidence of the dispersion curves of the plate and cylindrical tube having the same wall thickness, for large values of $|pR| < |qR|$; $|pR| \to \infty$ meaning large mean radius of the tube and/or high frequencies.